SAND2020-5102C
Proceedings of the ASME 2020
International Design Engineering Technical Conferences
and Computers and Information in Engineering Conference
IDETC/CIE2020
August 16-19, 2020, St. Louis, MO, USA

DETC2020-18809

METAMATERIAL DESIGN FOR TARGETED LIMB-SOCKET INTERFACE PRESSURE OFFLOADING IN TRANSTIBIAL AMPUTEES

Nathan Brown[1], Meredith K. Owen[2], John D. DesJardins[2], Anthony Garland[3], Georges M. Fadel[1]
[1]Department of Mechanical Engineering, Clemson University, Clemson, SC
[2]Department of Bioengineering, Clemson University, Clemson, SC
[3] Center for Integrated Nanotechnologies, Sandia National Laboratories, Albuquerque, NM

ABSTRACT

While using a prosthesis, transtibial amputees can experience pain and discomfort brought on by large pressure gradients, at the interface between the residual limb and prosthetic socket. Current prosthetic interface solutions attempt to alleviate these pressure gradients by using soft homogenous liners to reduce and distribute pressures. This research investigates an additively manufactured metamaterial inlay with adjustable mechanical response in order to reduce peak pressure gradients around the limb. The inlay uses a hyperelastic behaving metamaterial (US10244818) comprised of triangular pattern unit cells which can be 3D printed with walls of various thicknesses controlled by draft angles. The hyperelastic material properties are modeled using a third order representation based on Yeoh 3rd order coefficients. The 3rd order coefficients can be adjusted and optimized to represent a change in the unit cell wall thickness to create an inlay that can meet the unique offloading needs of an amputee. Finite element analyses evaluated the pressure gradient reduction from: 1) A common homogenous silicone liner, 2) A prosthetist's inlay prescription that utilizes three variations of the metamaterial, and 3) A metamaterial solution with optimized Yeoh 3rd order coefficients. When compared to a traditional homogenous silicone liner for two unique limb loading scenarios, the prosthetist prescribed inlay and optimized material inlay can achieve equal or greater pressure gradient reduction capabilities. These results show the potential feasibility of implementing this metamaterial as a method of personalized medicine for transtibial amputees by creating customizable interface solution to the meet unique performance needs of an individual patient.

Keywords: Prosthetics, Optimization, Elasticity, FEA, Metamaterials, Additive Manufacturing, Personalized Medicine

1. INTRODUCTION

A lower limb prosthesis provides increased ambulatory function for an amputee. The amputee should feel confident that the prosthesis provides the comfort and functionality needed to complete routine tasks [1]. Given that 84% of amputees wear the prosthesis an average of 12 hours a day, comfort is vital [2]. A prosthesis usually subjects the residual limb tissues to unnatural loading conditions, which can lead to discomfort, dermatological issues, deep tissue damage, and prolonged joint and muscle pain [3-7]. Understanding the pressure distributions around the limb is often the best way to understand how to counteract the discomfort experienced by lower-limb amputees [8]. Most studies show the largest stress concentrations can appear around the Patellar Tendon (PT), Tibial Crest (TC), Fibular Head (FH), and/or Tibial End (TE) [9-12], as referenced in Figure 1.

The magnitudes of the peak stress (PS) are often the focus of studies, as this stress is a key contributor to skin breakdown that can lead to many undesirable issues experienced by lower limb amputees. However, a determined range of pressure magnitudes that can predict this skin breakdown does not exist [13-14].

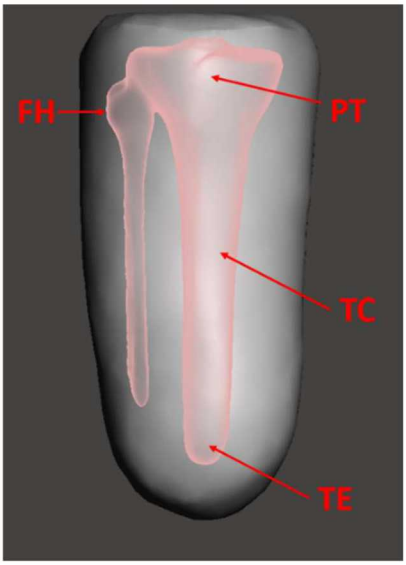

Figure 1. ANATOMICAL REPRESENTATION OF ANTERIOR RIGHT TRANSTIBIAL LIMB. PATELLAR TENDON (PT), FIBULAR HEAD (FH), TIBIAL CREST (TC) TIBIAL END (TE)

Sandia National Laboratories is a multimission laboratory managed and operated by National Technology & Engineering Solutions of Sandia, LLC, a wholly owned subsidiary of Honeywell International Inc., for the U.S. Department of Energy's National Nuclear Security Administration under contract DE-NA0003525.

Peak pressure gradient (PPG), instead of PS, may play a larger role in predicting residual limb issues. PPG is the spatial change in pressure at the limb surface, orthogonal to the normal vector pointing out from the residual limb, around the area of PS. These large pressure gradients contribute to skin breakdown because of the large shearing stresses placed on the soft tissues [15], which emphasizes the need to decrease the PPG as well as the PS on the surface of a residual limb.

Prosthetic liners are often implemented as an interface between the rigid socket and residual limb to transmit and distribute loads and reduce interface stresses [11]. Their main purpose is to alleviate the transfer of loads from the prosthetic socket to the residual limb. Prosthetists rely on personal intuition and experience when choosing the appropriate liner for a respective patient [5].

The first prosthetic liners were made from open and closed cell foams that were designed to encompass the residual limb [16-17]. Recently, silicone and elastomer liners replaced foams as the most commonly implemented pressure offloading solution because of increased durability and pressure distribution capabilities compared to foams [5, 18].

Prosthetic liner materials have been a common focus of research. *Sanders and Daly et al*. [16] altered the mechanical properties of foam liners through vacuum-forming manufacturing of foam liners. The vacuum forming weakens the cell structure. By controlling the degree by which these cell structures are weakened, Sanders proposed that the foam liners could be altered to fit the performance needs of specific patients [16].

In another study, *Sanders et al.* [19] investigated the compression stiffness and coefficient of friction of different liner materials. Spenco®, Poron®, silicone, soft pelite, medium pelite, firm Plastazote®, regular Plastazote®, and nickelplast were tested. The compression testing mimicked conditions the liner would experience within the prosthetic socket. The coefficient of friction was evaluated against both skin and sock. The results suggested that softer materials like regular and firm plastazote, and soft and medium pelite would be most advantageous around boney prominences, while the stiffer materials should be applied around the soft tissue. Materials with too low of a coefficient of friction were deemed unable to meet the suspension requirements needed in a prosthetic.

Boutwell et al. [12] focused on the thickness of gel liners as compared to the liner material itself. The study investigated the effects of gel liner thickness on peak socket pressures around the fibular head. Most of the subjects perceived increased comfort with a thicker liner. The increased comfort was linked with reduced fibular head stresses. The thicker liners were assumed to be more comfortable because of increased compliance. The authors proposed a thicker gel liner would reduce pressures around boney prominences as compared to thinner liners. Future research aims to determine optimal gel thicknesses for patients to provide a more customized solution to match the needs of the individual.

Klute et al. [5] Expressed concern that there is little scientific evidence to guide a prosthetist in the liner prescription process. Research shows that liners can help distribute pressures and can lead to increased comfort. However, there is limited evidence in the difference between the potential benefit of each material for specific patients.

Hafner et al. [20] looked to further understand the prosthetists' liner selection practices. The results of this survey driven study showed that the liner manufacturers were the primary source for information on available liner products. Liner characteristics like durability, comfort and suspension are often the driving factors in the selection of a liner. Even though there are more than 70 available liner solutions on the market, the study's respondents reported only having prescribed 16 of the 70 liners to their patients. Of those 16, the respondents said they routinely only used 2-3 liners to meet the needs of their patients. The most common liner materials of these prescriptions were silicone, thermoplastic elastomer, and urethane. The study concluded by emphasizing the need for an objective tool or resource to better pair individual patients with liner solutions that meet the unique performance needs of each amputee.

Nearly all transtibial amputee research has been limited to the use of homogenous material liners. A significant gap is apparent in the need to investigate non-homogenous liners. The research suggests that boney prominences should be offloaded by softer materials while soft tissue benefits from the suspension capabilities of stiffer materials. A homogenous liner would not be able to satisfy this recommendation. One method of achieving variable stiffness within a single inlay body would be the implementation of metamaterials.

Metamaterial research first originated in the field of optics [21-25] but eventually progressed to acoustics and mechanics. Mechanical metamaterials are man-made materials constructed from repeating unit cells or patterns which results in the mechanical properties of the metamaterial being a function of the base constitutive material and the unit cell or pattern design. [26] Metamaterials enable customization of their mechanical response through purposeful design of the unit cell parameters and selection of base constitutive material. By varying the unit cell parameters as a function of the 3D position within a bulk metamaterial, the properties at each location can be customized to best meet the design objectives of the metamaterial. Recent advances in additive manufacturing (also called 3D printing) enable printing a wider range of base materials (including elastomers) at a relatively low cost which enables fabrication of these metamaterials [27].

This paper investigates transtibial residual limb PPG reduction through the implementation of a metamaterial inlay for limb models targeting offloading at the FH, PT, and TE. Through finite element analysis (FEA), this investigation shows a reduction in the PPG when using a metamaterial liner when compared to a traditional homogenous material liner, and in the absence of a liner.

Clinically testing the limb stress distributions can be challenging due to cost, time, and patient recruitment and retention [28]. Therefore, a significant amount of prosthetic research is completed with the aid of FEA. FEA is a valid alternative to in vivo testing to determine the stress, strains, and

deformations of a residual limb [10-11, 29-34]. However, further research on human subjects or physical models would validate the current work. This validation is the subject of continuing research.

2. MATERIALS AND METHODS

2.1 Metamaterial Material Properties

Based on the recommendation from *Sanders et al.* [29], a method to implement an interface material between the residual limb and socket was sought, that could be soft at the boney prominences but stiffer around large concentrations of soft tissue. Members of the research team had previous experience working with a metamaterial with adjustable mechanical response (Patent US10244818 B2) [35] that had been used in orthotics to offload pressure for patients with diabetic foot ulcers. While the original application of this metamaterial was orthotics, the designers of this metamaterial saw the potential of implementation at other anatomical locations such as the hip, head, knee, hand, and chin, which sparked the interested in using this metamaterial for this study.

The metamaterial, seen in Figure 2, is constructed by 3D printing walls of various thicknesses controlled by draft angles. These various wall thicknesses leave a triangular patterned unit cell indented into the top surface of the base material. The pattern is comprised of four equal sized triangles spanning radially 180 degrees. This four-triangle base unit is patterned orthogonally. The base material is made of 100% TangoPlus (*Stratasys, Ltd, Eden Prairie, MN)*. All samples were additively manufactured using an Object Connex 350 3D printer. The Base Material is highly flexible and has a similar feel and appearance as rubber. For this study, the draft angles were limited to 0, 1.9, 4.1, 6.6, 9.7, 14.5, and 27.5 degrees. The material samples are referenced as DA_{00}, DA_{02}, DA_{04}, DA_{06}, DA_{09}, DA_{14}, and DA_{27} with the two digits subscript to "DA" corresponding to the approximate draft angle associated with the patterned unit cell. The seven draft angles were selected to provide a set of materials with discernable shore O hardness values. The hardness values of DA_{27} and the base material were similar enough to justify making 27.5˚ the largest draft angle. This metamaterial was original designed for changes in hardness to mimic changes in the metamaterial's mechanical response. The correlation between hardness and changes in mechanical response are not directly proportional, but, in a relative sense, a low hardness value correlates to a smaller required force to reach a desired material deformation and vice-versa [35]. The change in draft angle alters fill volumes of the voids, and thus the thickness of the walls between each cell, which in turn affects the mechanical response of the material as a whole, as seen in Figure 2D.

To develop material models for the metamaterial variations, 60mm by 60mm samples (n=3) of each draft angle variant metamaterial were tested in uniaxial compression, using an ADMET eXeprt 5601 testing system (*ADMET, Norwood, MA)*. The compression plate measured 203mm by 203mm and therefore covered the entirety of the testing sample. The testing followed ASTM D575 standards for all components of rubber

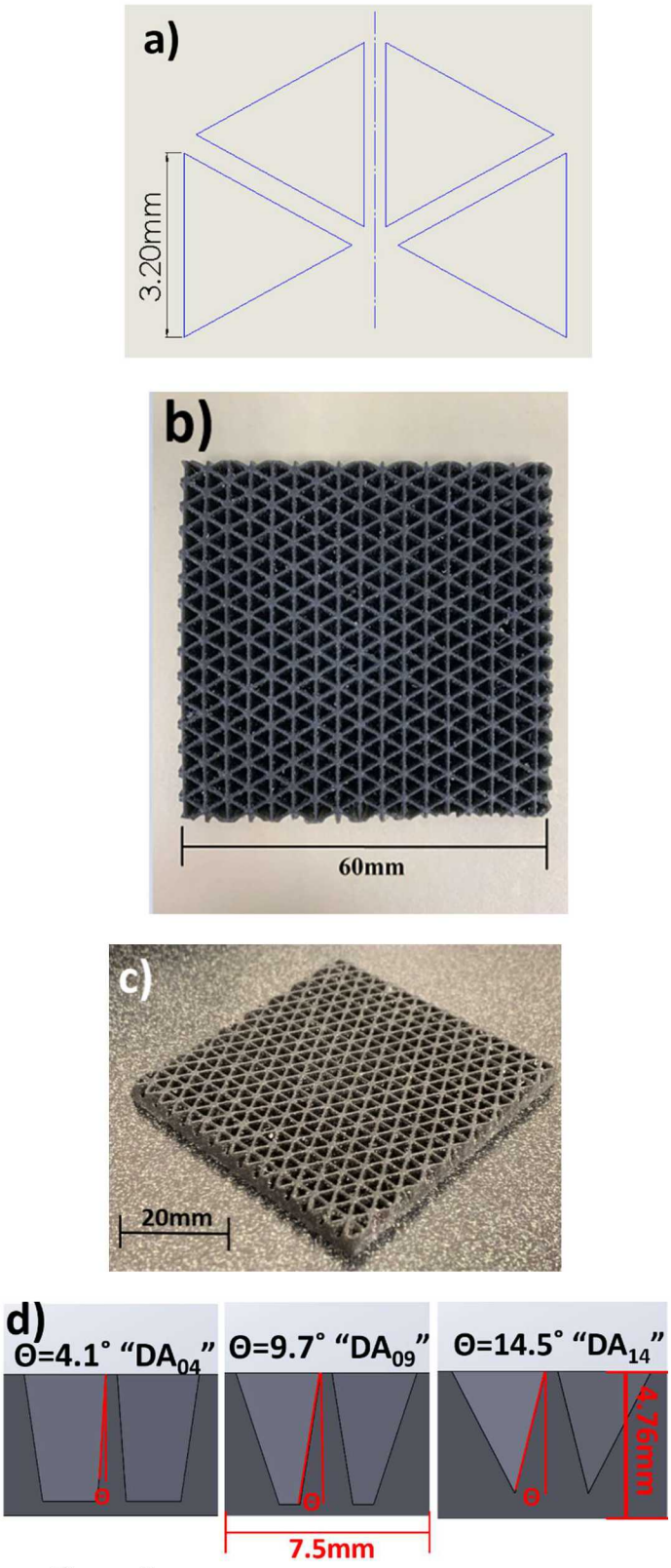

Figure 2. a) TRIANGULAR UNIT CELL b) TOP VIEW OF PATTERNED UNIT CELLS c) ISOMETRIC VIEW d) SECTION-VIEW OF WALL THICKNESS COMPARISON OF INDIVIDUAL UNIT CELLS

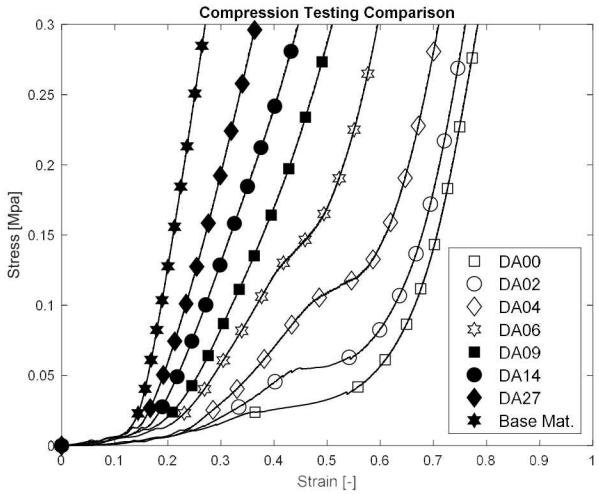

Figure 3. STRESS-STRAIN CURVES PRODUCED FROM EXPERIMENTAL COMPRESSION TESTING

material testing besides the thickness of the test specimen. ASTM D575 calls for a slab approximately 13mm in thickness. However, the metamaterial in this study is designed to be approximately 4.76mm in thickness for use in the inlay and therefore the deflection rate of the plate was altered from 12mm/min to 4.4mm/min. Three samples of each material were tested to account for material property variability that can arise over time from this composition [36]. *Sanders et al.* [19] utilized this quasi-static method of material compression testing with prosthetic liner materials and determined that these methods were viable to represent the in vivo conditions a liner would undertake.

The stress-strain curves, seen in Figure 3, show the variable material properties that can be achieved through the altering of the draft angle. Each material shows hyperelastic behaving material properties. The smaller wall thicknesses that arise from the lower draft angles lead to a more drastic buckling during compression. The buckling is represented by the noticeable reduction in slope between 40% and 60% strain of the stress-strain curves for DA_{00}, DA_{02}, DA_{04}, and DA_{06}.

A material model was needed in order to provide simplified representations of the experimental stress-strain curves. A range of hyperelastic material models can be used to model the non-linear deformation of a material. The hyperelastic materials are described through a strain-energy function. The strain-energy density can be used to derive the relationship between the stresses and strains of a material during deformation. The non-linear relationship between the stresses and strains are defined through a series of material parameters. High order material models have more material parameters which may more accurately describe the stress-strain relationship, but they also increase the complexity of the material model. The material parameters are selected so that the model best matches the experimental stress-strain results [37]. For this research, the selected material model needed to accurately represent the experimental data while limiting the number of material parameters. Using a tool within *ANSYS® Academic Research Mechanical, Release 19.2*, the accuracy and simplicity of several material models were tested, and a Yeoh 3rd order representation was selected to model the compression testing results. The three Yeoh material coefficients (Table 1) were found such that, when plugged into Eq 1 [37], the model best matched the compression testing data of the given material. The third order graphical representations of each material can be seen in Figure 4.

$$\sigma = \sum_{i=1}^{3} 2iC_{i0}[(1+\varepsilon) - (1+\varepsilon)^{-2}][(1+\varepsilon)^2 + (2(1+\varepsilon)^{-1} - 3)]^{i-1} \quad (1)$$

The R^2 values in Table 2 show the calculated Yeoh 3rd order coefficients are valid approximations of the inlay materials.

Table 1. YEOH 3RD ORDER MATERIAL COEFFICIENTS OF EACH METAMATERIAL AND BASE COMPOSITE MATERIAL

	C_{10} [Pa]	C_{20} [Pa]	C_{30} [Pa]
DA_{00}	3225	95778	32987
DA_{02}	646	1.599E5	42500
DA_{04}	1846	1.877E5	2.855E5
DA_{06}	1760	79549	-7016
DA_{09}	3260	66206	-11759
DA_{14}	839	23329	2455
DA_{27}	1271	6326	9544
Base Mat.	446	88326	2.510E6

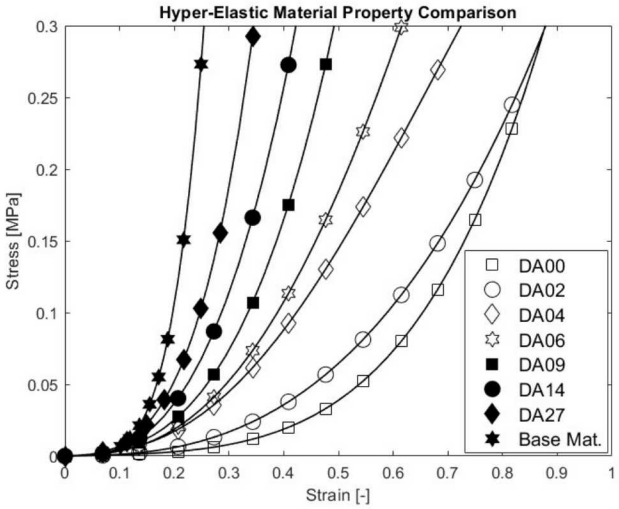

Figure 4. STRESS-STRAIN CURVES PRODUCED FROM YEOH 3RD ORDER MATERIAL COEFFICIENTS

Table 2. R^2 VALUES FOR MATERIAL COEFFICIENTS WITH RESPECT TO COMPRESSION TESTING RESULTS

DA_{00}	DA_{02}	DA_{04}	DA_{06}	DA_{09}	DA_{14}	DA_{27}	Base Mat.
0.908	0.904	0.921	0.986	0.990	0.978	0.974	0.947

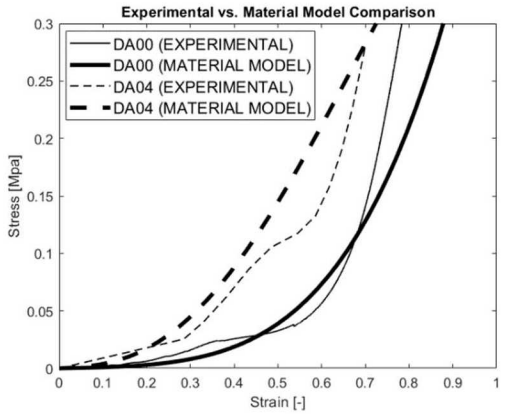

Figure 5. STRESS-STRAIN COMPARISON OF EXPERIMENTAL COMPRESSION TESTING AND 3RD ORDER MATERIAL REPRESENTATION OF DA_{00} AND DA_{04}

The R^2 values represent how closely the experimental compression testing results fit with the Yeoh 3rd order representation. The biggest limitation for this third order representation is properly representing the drastic buckling experienced by lower draft angle materials, as represented in Figure 5. These materials have a lower R^2 value because the third order material model cannot properly represent the drastic buckling reaction. Materials with larger draft angles, like DA_{06} and DA_{09}, are not subject to as severe wall buckling which means they can be more accurately represented using third order coefficients, which is apparent by the larger R^2 values. The reasoning for why the base material and DA_{27} vary from the trend of a larger draft angle leading to a higher R^2 value is unknown.

2.2 FEA Set Up

The FEA was set up to mimic the in vivo conditions of a transtibial amputee. Two different limb shapes were evaluated. The limb models were taken from 3D scans of two deidentified transtibial amputees. The limb shapes were obtained as part of an Institutional Review board approved study. The first limb shape (L1) represented an approximately 180-pound, 5-ft 6-in transtibial amputee requiring pressure offloading at the FH. The second limb model (L2) represented an approximately 240-pound, 6-ft 4-in transtibial amputee, requiring offloading at the PT and TE. Both limb models had a conical shape with no abnormal protrusions.

Each limb model underwent a series of FEA to compare the PS and PPG on the surface of the residual limb under four conditions: 1) No liner 2) A Homogenous Silicone Gel liner 3) A practitioner prescribed inlay utilizing the metamaterials 4) A metamaterial solution with optimized Yeoh 3rd order coefficients. The Silicone Gel liner is one of the most popular current liner solutions for transtibial amputees and provides an appropriate comparison target for the metamaterial inlay [20].

The tibia and fibula models were sized, formed, and placed within the limb models based on recommendations from *McGrath et al* [38]. A bone cavity was formed inside the limb using *SOLIDWORKS 2018*. The inlay was constructed by isolating the exterior surface of the limb corresponding to the inlay shape and extruding it approximately 4.76mm in the normal direction to the residual limb. This method ensures that the inlay and limb remain flush against each other to mimic the interaction of an in vivo limb and inlay. The shapes of the inlays were derived from a clinical prosthetist's recommendation. The prosthetic socket was formed by scaling the limb to envelop the entire inlay and limb. A cavity was formed using *SOLIDWORKS 2018* to ensure that the inlay and limb remain flush against the socket, creating a Total Surface Bearing socket (TSB). *Zheng et al.* [39] implemented a similar method and yielded accurate results. This process was repeated for both limb shape simulations. Figure 6 shows the difference between models used for the two limb shapes. To simplify the analysis for L1, the model was reduced to target just the areas around the FH (Figure 7). This simplification drastically reduces the computational time of the simulation. The full limb model was necessary for L2, due to specific offloading locations.

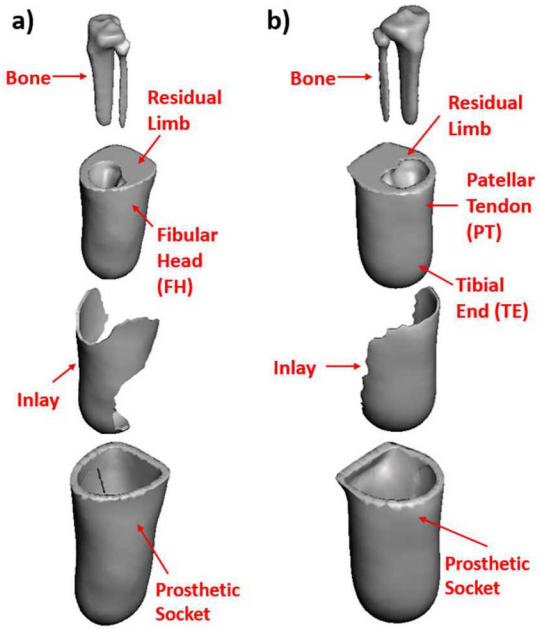

Figure 6. STL. EXPLODED MODEL FOR a) L1 b) L2 (THE TOP SURFACE OF THE LIMB AND SOCKET HAVE BEEN REMOVED FOR CLARITY)

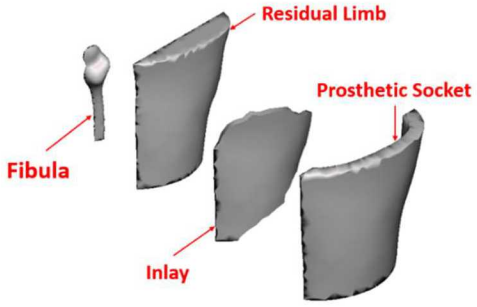

Figure 7. ISOLATED FH EXPLODED VIEW FOR L1

The tibia and fibula models were modeled with a linear elastic material with an elastic modulus of 15 GPa and Poisson's ratio of 0.3. The prosthetic socket was modeled as polypropylene with a linear elastic modulus of 1.5 GPa and Poisson's ratio of 0.3 [25]. The limb model was modeled homogenously as soft tissue. The hyperelastic material properties of soft tissue can be modeled using Yeoh 3rd order with C_{10}= 0.004154, C_{20}= 0.050753, C_{30}= -0.013199 MPa [40]. For the "No Inlay" conditions, the inlay was modeled as polypropylene. Several studies have shown that silicone liners can be accurately modeled linearly with a modulus of elasticity of 0.35 MPa and Poisson's ratio of 0.3 [33]

Based on subject matter expertise and patient input, the prosthetists selected metamaterial variations and their corresponding layouts to design the inlay. The prosthetists had not worked with this metamaterial before and therefore did not have the experience needed to help guide the prescription. For L1, the practitioner prescribed an inlay (Figure 8) that included three materials (DA_{09}, DA_{14}, and DA_{27}) with circular offloading of set radii around the fibular head. The prescription set DA_{09} as an internal circular region that transitions to a region of DA_{14} internally and externally bounded by the dimensions seen in Figure 8. The remaining portions of the inlay are set as DA_{27}. The regions of DA_{09}, DA_{14}, and DA_{27} set by the dimensions in Figure 8 are referenced as the "FH Inner Material", "FH Middle Material", and "FH Outer Material", respectively, in later optimization results for the FH.

For L2, the practitioner prescription (Figure 9) targeted the PT and TE as regions of offloading. The patellar tendon only requires sections of DA_{14} and DA_{27}. The DA_{14} region is set by the parameters in Figure 9A. This offloading mainly targets the PT through the use of an ellipse layout of DA_{14} and extends down to the TC. The regions of DA_{14} and DA_{27} set by the dimensions in Figure 9A are referenced as the "PT Inner Material" and "PT Outer Material", respectively, in later optimization results for the PT. The TE prescription includes DA_{09}, DA_{14}, and DA_{27}. The internal and external ellipses are bounded by the dimensions in Figure 9B. The internal and external ellipses were made of DA_{09} and DA_{14}, respectively. The remaining regions of the inlay are represented by DA_{27}.The regions of DA_{09}, DA_{14}, and DA_{27} set by the dimensions in Figure 9B are referenced as the "TE Inner Material", "TE Middle Material", and "TE Outer Material", respectively, in later optimization results for the TE. It should be noted that, within the FEA, the metamaterials were represented by solid bodies assigned the Yeoh 3rd order coefficients presented in Table 1. This method ensures that the respective metamaterial regions of the inlay behave similarly to the metamaterials in a physical model.

For all simulations, the exterior surface of the prosthetic was held as the fixed support. For L1, a load of 60N was applied to the flat face of the isolated fibula. L2 was loaded with 1090 N of compression and 205 N of anterior-posterior shear. These loading conditions are set to mimic the largest loading conditions the limb might experience during the gait cycle given the weight of the subject [38]. This quasi-static loading representation of the

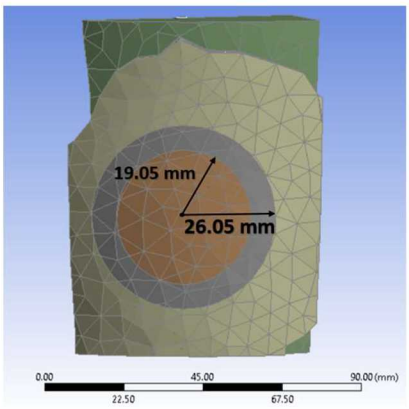

Figure 8. LIMB SHAPE 1 PROSTHETISTS PRESCRIBED INLAY (PROSTHETIC SOCKET REMOVED FOR CLARITY)

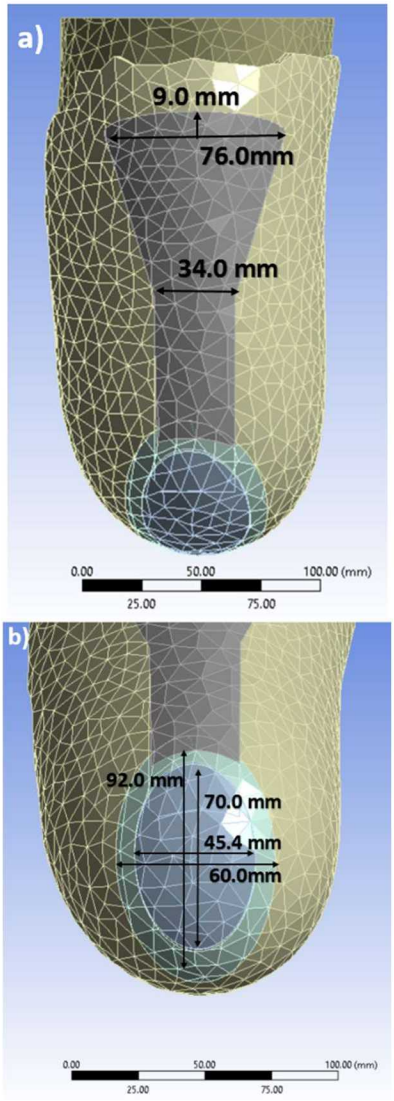

Figure 9. LIMB SHAPE 2 PROSTHETISTS PRESCRIBED INLAY a) TARGETTING THE PATELLAR TENDON b) TARGETTING THE TIBIAL END (PROSTHETIC SOCKET REMOVED FOR CLARITY

dynamic nature of an amputee in the gait cycle has been validated by *Faustini et al.* [41] who utilized quasi-static loading conditions derived from experimentally measured ground reaction forces to mimic in vivo testing within FEA.

The coefficient of friction (COF) between the limb and socket, as well as the inlay and socket, were set to μ=0.5. The COF between the inlay and limb is approximately 2.0 and therefore they were modeled as being bonded [22]. A mesh convergence study was run on the No Inlay condition on L1 and L2 and a maximum mesh element size of 2.0mm was deemed the appropriate selection for both models. This element size ensures that even the most finite critical components, such as the thickness of the inlay, have enough mesh details to accurately evaluate the results.

3. RESULTS AND DISCUSSION

3.1 Limb Shape 1 Results

Equivalent Von-Misses stresses on the surface of the residual limb were determined for each condition. Figure 10 is an example of a visual representation of the results which were used to determine the PS and PPG for each evaluation**.** Results for each condition from L1 are summarized in Table 3. The effectiveness of each liner type was judged based on its gradient reduction capabilities relative to the "No Inlay" condition. The practitioner prescribed inlay and silicone liner conditions provide a reduction in both the PS and PPG. The PPG reduction abilities of the silicone liner and practitioner prescribed inlay are nearly identical, while the PS was reduced more using the silicone liner as compared to the practitioner prescription.

3.2 Limb Shape 1 Optimization

The next step is to optimize the material properties to further investigate the offloading capabilities of the metamaterials. The three Yeoh material coefficients of the three materials were set as optimization parameters. Optimizing the material coefficients is meant to act as a representation of optimizing the draft angle of the metamaterial. The idea of altering key parameters to guide the redesigning of unit cells was proposed by *Satterfield et al.* [42] who determined that altering parameters that represent the physical response of a unit cell can lead to similar results as altering the unit cell directly.

Reduction of PPG on the limb surface is the goal of the optimization. Finding an analytical equation which directly links reduction in PPG with design variables is difficult. Therefore, this optimization problem looks to minimize an approximation of the PPG. An ideal liner would cause homogenous limb surface stress, meaning the maximum and average limb stress would be equal. Therefore, to minimize the PPG, the objective of the optimization was set to minimize the difference between the maximum and average limb surface stress. An adaptive single-objective method, a variant of the popular NSGA-II (Non-dominated Sorted Genetic Algorithm II), was used and described as:

$$Obj = \min\left|\left(Stress_{max} - Stress_{avg}\right)\right| \qquad (2)$$

Design Variables: $C_{10-Inner}$, $C_{10-Middle}$, $C_{10-Outer}$, $C_{20-Inner}$, $C_{20-Middle}$, $C_{20-Outer}$, $C_{30-Inner}$, $C_{30-Middle}$, $C_{30-Outer}$

s.t.

$$0\ Pa < C_{10-Inner}, C_{10-Middl}, C_{10-Outer} < 1E4\ Pa$$
$$0\ Pa < C_{20-Inner}, C_{20-Middle}, C_{20-Outer} < 5E5\ Pa$$
$$0\ Pa < C_{30-Inner}, C_{30-Middl}, C_{30-Outer} < 5E5\ Pa$$

The bounds of the optimization were set based on the original values of C_{10}, C_{20}, and C_{30} in Table 1.

Each optimization was set to run with 40 initially assigned samples and generate 10 updated samples every iteration until the 2% convergence stability was met. The optimization around the FH utilized *ANSYS* direct optimization, which took 140 FEA calls to converge, each taking slightly longer than 5 minutes through the utilization of 24 cores with 128 GB of RAM on Clemson University's Palmetto Cluster. The optimized material coefficients in Table 4 were used to represent the optimized coefficient inlay condition.

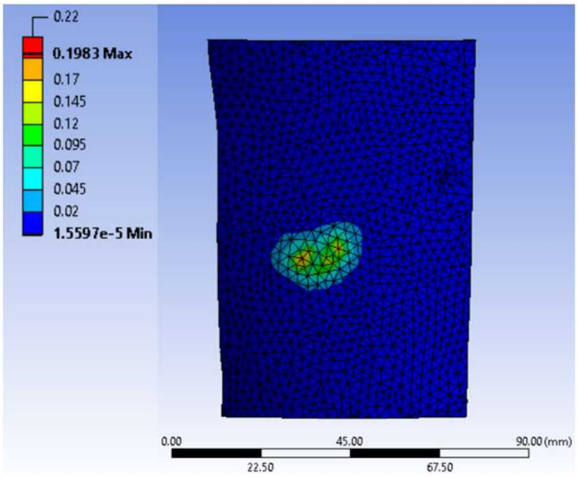

Figure 10. LIMB SURFACE STRESSES FOR "NO INLAY" SIMULATION [MPa]

Table 3. PEAK STRESS & PEAK PRESSURE GRADIENT COMPARISON FOR LIMB SHAPE 1

Liner Type	Peak Stress (PS) [MPa]	Peak Pressure Gradient (PPG) [kPa/mm]	Gradient Reduction Compared to "No Inlay"	PPG:PS
No Inlay	0.198	32.4	-	163.7
Silicone Liner	0.134	22.0	32.1%	164.2
Prosthetists Prescription	0.175	22.1	31.5%	126.3
Opt. Material Coefficients	0.100	13.8	57.4%	138.0

Table 4. OPTIMIZED YEOH 3RD ORDER COEFFICIENTS AROUND THE FIBULAR HEAD [FH]

	FH Inner Material	FH Middle Material	FH Exterior Material
C_{10} [Pa]	8988	3877	4559
C_{20} [Pa]	5019	3.297E5	3.487E5
C_{30} [Pa]	16937	2.577E5	2.834E5

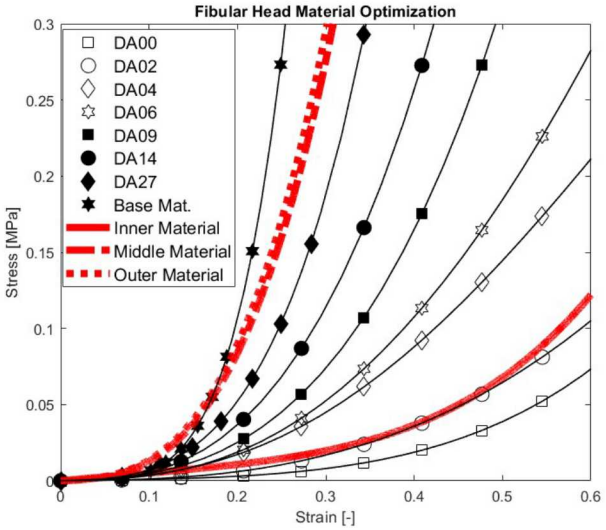

Figure 11. SS COMPARISONS OF OPTIMIZED MATERIAL PROPERTIES AND TESTED METAMATERIALS. OPTIMIZED MATERIAL IS SHOW IN RED AS INNER MATERIAL, MIDDLE MATERIAL, AND OUTER MATERIAL

The "Opt. Material Coefficients" results in Table 3 shows a further reduction in PS and PPG are possible beyond the practitioner prescribed inlay condition.

To better understand the physical meaning of the optimized material coefficients, the stress-strain curves were produced utilizing Eq 1 and compared to the stress-strain curves of the current third order representations of the metamaterial (DA_{00}-DA_{27} and Base material). These stress-strain curves allow for a visual comparison between the optimized material properties and how they behave relative to the third order representations of the metamaterials with predetermined draft angles. This comparison will give insight into what draft angle the optimized metamaterial should be printed at to achieve the desired pressure gradient reduction. The results indicated in Figure 11 show that the internal material should have a draft angle much lower, between DA_{02} and DA_{04}, then the current prescription, while the middle and exterior surfaces should have draft angles somewhere between DA_{27} and the base material.

3.3 Limb Shape 1 Discussion

Previous research shows a range of accepted peak limb stresses in both the simulation and clinical settings [10-11, 29-34]. When adjusted for the weight of the patient, the results of the "No Inlay" condition simulation are within one standard deviation of the clinical results on the FH, 1.82 kPa/kg (.88) found by *Yeung et al.*[43], validating the assumptions and approximations made in this model to mimic in vivo conditions.

Table 3 shows that the introduction of an interface material decreases the PS and PPG as expected. Each of the interface solutions are more compliant than the prosthetic socket and therefore the liner deformation caused by the limb is much larger than the socket. The increased deformation allows the force to be distributed over a larger area and therefore the PS is reduced [12]. The silicone liner has a smaller PS compared to the prosthetist's prescribed inlay because the silicone material around the FH was modeled as a softer material compared to the internal material of the prosthetists prescribed inlay, DA_{09}. The prosthetist's prescription has a near identical PPG as the silicone liner which is interesting considering the PS is several kPa's larger. The similar PPG of the prosthetist's prescription and silicone liner can be accredited to the gradual mechanical response change of the metamaterial variations within the prosthetist's prescription. As *Klute et al.* recommended, the softer DA_{09} was located on the boney FH while DA_{14} and DA_{27} were located on the soft tissues, allowing for a less drastic reduction in pressure [5].

The optimized material coefficients make the internal material softer than silicone, allowing for greater deflection of the inlay around the boney prominence, which further reduces the PS and PPG. Figure 11 shows the middle and exterior material properties are very similar and both show a mechanical response between DA_{27} and the base material, suggesting that proper offloading of the FH could be achieved with just two materials. The optimization results also show that the prosthetist's recommendation of DA_{27} as the outer material was closer compared to the recommendation of DA_{09} as the inner-most material.

As previously discussed, the goal of this study was to reduce the PPG on the limb surface, not just the PS. The inlay is designed to directly target the reduction of the PPG as compared to just aiming to reduce PS with a reduction in PPG as a byproduct. In order to validate this claim, the ratio between PPG and PS has been included in Table 3. These results show that the ratio between PPG and PS are not identical for all conditions. This means that the reductions of PS and PPG are not linearly correlated. In fact, a reduction in this ratio is desirable because it indicates that the PPG is being reduced at a greater rate compared to the PS. The PPG:PS ratio for the prosthetist's prescription and optimized material coefficients conditions are both smaller than the No Inlay or Silicone liner ratios which shows that the metamaterial inlay does a better job at directly targeting the reduction of the PPG. The lowest ratio results from the prosthetist's prescription show that this inlay configuration does the best at directly targeting the PPG. This does not mean that the prosthetists prescription will deliver the most comfort to the patient. It just shows that the metamaterial inlay is more directly targeting the reduction of the PPG instead of simply a byproduct of PS reduction. The optimized material coefficients will prove the most comfortable solution as it is able to achieve the greatest reduction in PPG, which is the ultimate goal.

3.4 Limb Shape 2 Results

The PS and PPG comparisons were targeted at the PT and TE for L2, which were determined from visual representations of the limb surface stress like the results seen in Figure 12. The results in Table 5 show that the introduction of an interface material around the TE will both reduce the PS and PPG. The practitioner prescribed inlay has greater gradient reduction capabilities compared to the silicone liner conditions at the TE. The results at the PT show that the silicone liner increased the PS and PPG while the practitioner prescribed inlay again reduced both components.

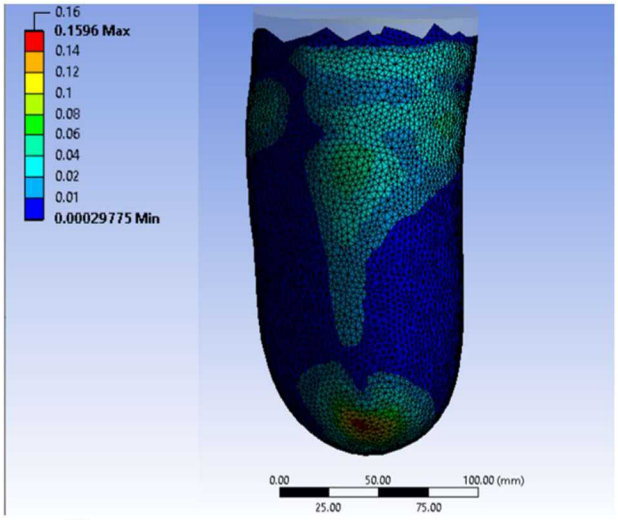

Figure 12. LIMB SURFACE STRESS FOR "No Inlay" CONDITIONS [MPa]

Table 5. PEAK STRESS AND PEAK PRESSURE GRADIENT COMPARISON FOR LIMB SHAPE 2 FOR TIBAIAL END (TE) AND PATELLAR TENDON (PT)

Limb Area	Liner Type	Peak Stress [MPa]	Peak Pressure Gradient [kPa/mm]	Gradient Reduction Compared to "No Inlay"	PPG:PS
TE	No Inlay	0.160	16.9	-	105.6
	Silicone Liner	0.122	7.59	44.9%	62.2
	Prosthetists Prescription	0.079	5.88	65.2%	73.4
	Opt. Material Coefficients	0.069	5.16	69.5%	74.8
PT	No Inlay	0.053	2.33	-	44.0
	Silicone Liner	0.076	3.23	-38.6%	42.5
	Prosthetists Prescription	0.035	1.76	24.5%	50.3
	Opt. Material Coefficients	0.036	1.50	35.6%	41.7

3.5 Limb Shape 2 Optimization

The optimization for L2 had the same objective (Eq 2) and parameter bounds as L1. Two separate optimization evaluations were run to target the TE and PT, individually. The limb surface area was broken into two regions in order to isolate the areas around the TE and PT. Following the prosthetist's recommendation, the optimization for the PT only required two materials (6 coefficients) while the TE required three materials (9 coefficients). Again, *ANSYS* direct optimization was utilized to run the optimization problem. The optimization around the TE and PT took 220 and 150 FEA calls, respectively. Each simulation took approximately 18 minutes utilizing the same resources from the Palmetto Cluster. The coefficient results from Table 6 were used to represent the optimized condition. The "Opt. Material Coefficients" inlay results from Table 5 show that the optimized material coefficients resulted in the smallest PS and the largest percent reduction in PPG.

The stress-strain curves were created to compare the physical behaviors of the optimized coefficients to the currently selected materials. Figure 13A shows that the internal material around the TE should have a draft angle much lower than the current DA_{09}. In fact, the draft angle should be between DA_{02} and DA_{04}. The middle and exterior materials should have a draft angle between DA_{27} and the base material. Unlike L1, the middle and exterior materials around the PT are distinct enough to justify the need to utilize a three-material approach to offload the TE. The two materials used to offload the PT should have similar mechanical responses compared to the base material. It should be noted that the "Strain Axis" of each optimized material SS curve has been adjusted accordingly to the maximum deflection of the inlay around the respective limb area.

3.6 Limb Shape 2 Discussion

The maximum stress values around the PT and TE for the "No Inlay" condition fall within one standard deviation of the clinical results found by *Yeung et al.* [43] when adjusted for patient weight. These results were 1.95 (1.49) kPa/kg and 1.51 (1.27) kPa/kg for the PT and TE, respectively.

Table 6. OPTIMIZED YEOH 3RD ORDER COEFFICIENTS FOR TIBIAL END (TE) AND PATELLAR TENDON (PT)

Limb Area	Coefficient	TE Inner Material	TE Middle Material	TE Exterior Material
TE	C_{10} [Pa]	1270	3058	9699
	C_{20} [Pa]	17340	2.993E5	4.244E5
	C_{30} [Pa]	37423	2.371E5	4.761E5
		PT Inner Material		PT Exterior Material
PT	C_{10} [Pa]	7537	-	9760
	C_{20} [Pa]	3.877E5	-	4.904E5
	C_{30} [Pa]	3.382E5	-	4.899E5

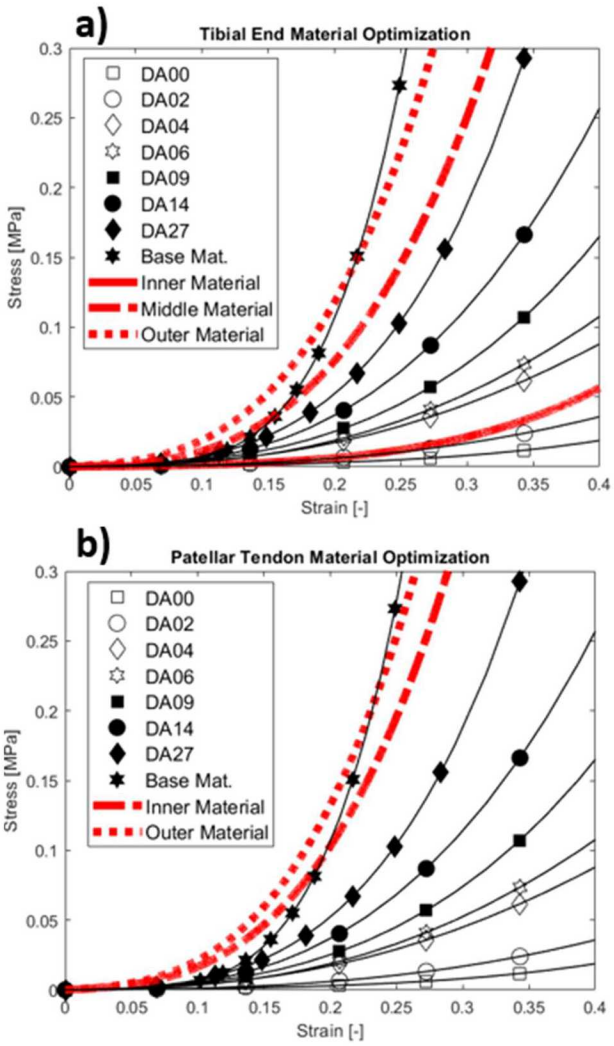

Figure 13. SS COMPARISONS OF OPTIMIZED MATERIAL PROPERTIES AROUND THE A) TIBIAL END B) PATELLAR TENDON. OPTIMIZED MATERIAL IS SHOW IN RED AS INNER, MIDDLE (IF APPLICABLE), AND OUTER MATERIAL

Table 5 shows the results around the TE for L2 are like L1 in that all liner solutions lead to a reduction in PS and PPG. The difference arises in that the practitioner prescribed inlay has a greater reduction in both PS and PPG. This variance from the L1 results is expected because of the combined loading situation of L2. Whereas L1 only experienced a normal force, L2's loading situation was a combined loading of normal and shear forces. At the TE, the larger 1090 N acts as the normal force, while the smaller 209 N acts as a shear force. The opposite occurs around the PT. With the introduction of a shear force, a softer material does not guarantee a smaller PS. *Sanders et al.* [19] proposed that a material with a lower shear stiffness allows the residual limb to move deeper into the socket upon weight-bearing, while one with a larger shear stiffness would not. The increased deflection into the socket can lead to an increased shear stress, increasing the magnitude of the equivalent stress. The increased shear stresses cause the PS and PPG around the TE of the silicone liner with a lower shear stiffness to be greater than the practitioner prescribed inlay with a higher shear stiffness.

The effect of shear stress is even more apparent around the PT where the PS and PPG values are increased with the introduction of the silicone liner compared to the "No Inlay" condition. The larger shear force exposed to the PT caused the majority of the load to be taken on by the soft tissue. The soft tissue then experiences a drastic increase in shear stress which increases the magnitude of the PS. The softest material in the practitioner prescribed inlay around the PT is DA_{14} which is significantly stiffer than silicone. This material difference reduces the deflection of the inlay, as well as limits the shear stress on the limb, explaining the reduction in PS and PPG with the practitioner prescribed inlay condition.

The optimized material coefficients for the TE slightly stray from the explanation above. The softest optimized coefficients are much softer than silicone. Additional FEA results show a greater inlay deflection around the "Inner Material" region of the optimized inlay compared to the silicone liner. Table 5 shows that the optimized coefficient solution can achieve the smallest PS and PPG even with an internal material softer than silicone. The explanation for this result may come from the multi-material approach. The "Middle Material" and "External Material" regions have a higher shear stiffness than silicone and in turn can help limit the shear force experienced by the soft tissue at the TE. Additional FEA results show that the shear stress around the "Inner Material" region of the PT is lower for the optimized coefficient inlay compared to the silicone liner, which validates the assessment that the multi-material solution can limit the total shear stress and therefore equivalent stress.

The optimized coefficient results for the PT do follow the claim that stiffer materials are better suited under high shear forces. The optimized coefficients cause the materials to be stiffer than the silicone liner and the prosthetist's prescribed inlay. These materials ensure that the liner deformation is limited to reduce the shear stress experiences on the limb, allowing for the PS and PPG to be reduced.

Regardless of the interface solution, the PPG:PS ratio is reduced relatively similarly around the TE. The silicone liner does have the lowest ratio which may indicate that the homogenous solution may be better suited to directly target PPG reduction in this combined loading situation compared to the metamaterial inlay.

The PPG:PS ratio results around the PT show very little difference between each of the conditions. This shows the reduction of PPG around the PT is more closely correlated with the reduction of PS. It should be restated that this ratio result for both the TE and PT are only used to indicate the inlay's ability to directly reduce PPG. This is not a direct correlation to the comfort of the inlay, which is better represented through the magnitude of the PPG.

3.7 Clinical Relevance Discussion

The assumptions and approximations presented in this paper may explain the difference between the results presented and published clinical results. The location of the areas of loading were not identical to in vivo reactions of the residual limb. *Lin et al.* [11] determined that so long as the loaded nodes are far enough apart to cover most of the superior bone surface, the effect of the location variance between FEA and clinical testing would be minimal.

The soft tissue was treated uniformly around the entire limb, which does not account for potential differences between muscle, fat, skin, and scar tissues present in the limb. These differing stiffnesses could alter the current results. The two limb models represent non-traumatic amputations and therefore it was expected that tissue distribution would be anatomically similar in the limb, which may not be the case in evaluations of other amputees.

A difficult part of achieving comfort within the prosthetic is the patient reaction. An inlay could be designed to minimize the PS and PPG but if the patient does not feel comfortable then the solution is unviable. One area of potential concern could be the drastic change in mechanical response between materials. This change could be felt as a rigid point on the inlay, potentially explaining why the prosthetists prescribed a three-material solution for the FH and TE for the respective limb shapes. The prosthetists anticipated that the transition between DA_{09} to DA_{14} and DA_{14} to DA_{27} is gradual enough to avoid a negative reaction from the patient. Care must be taken when applying the optimized material property results in a clinical setting to ensure that the material changes are not too severe to warrant a patient complaint. Even so, socket comfort is highly subjective for each patient [44-46] and can be very difficult to mathematically determine if an optimized inlay solution will satisfy the patient.

Another area of concern is selecting a metamaterial that a patient considers too soft. Experience has shown that patients can label materials that are too soft as “squishy”. This negative reaction will affect a patient’s confidence that the inlay will be able to hold up to the rigors required to provide comfort and stability to the amputee. Unfortunately, an acceptable material range will be highly subjective for each patient. Therefore, patient input would be necessary to determine if a selected metamaterial is too soft. A method to reduce the chances of the patient finding the selected metamaterial too soft is to add a constraint on the maximum deflection of the inlay to the optimization problem. This added constraint will ensure that the inlay has material properties that can provide enough rigidity to instill confidence into the amputee.

While these patients need to be considered, this research has introduced an additional tool that prosthetists can use during the prescription process. Implementing optimization into the prescription process will make it easier to meet the unique performance needs of an amputee. The design of patient specific inlays will still require prosthetists input to provide an initial prescription, but employing methods used in this research improve the chances that the amputee is fitted with a more comfortable solution in a shorter amount of time.

Further research should investigate the potential to optimize the layout of the materials as well as optimizing the material coefficients. The dimensional values of Figure 8 and Figure 9 along with the material coefficients could be changed to design variables. The objective would continue to focus on minimizing PPG.

4. CONCLUSION

The presented research has shown that a single layer metamaterial can reduce limb surface pressure in a transtibial prosthesis. The metamaterial representation was shown to reduce peak stress and peak pressure gradients greater than a common Silicone liner solution around three key locations of the residual limb, suggesting that heterogeneous material property liners are better equipped to increase comfort for amputees through reduction of PS and PPG. The hyperelastic material properties of this single layer metamaterial can be represented by three customizable material properties. The material properties can be optimized to meet unique performance needs of an amputee. The resulting optimized coefficients offer insight into how the metamaterial geometric parameters should be designed for an individual patient. This method has the potential to lead to a customized inlay solution to increase comfort and functionality within a prosthetic socket.

ACKNOWLEDGMENTS

The authors would like to acknowledge Brian Kaluf from Ability Prosthetics and Orthotics, Inc. for his clinical insight and expertise. The authors would also like to acknowledge Clemson University for the generous allotment of compute time on the Palmetto cluster.

This work was performed, in part, at the Center for Integrated Nanotechnologies, an Office of Science User Facility operated for the U.S. Department of Energy (DOE) Office of Science. Sandia National Laboratories is a multi-mission laboratory managed and operated by National Technology & Engineering Solutions of Sandia, LLC, a wholly owned subsidiary of Honeywell International, Inc., for the U.S. DOE’s National Nuclear Security Administration under contract DE-NA-0003525. This work was partially funded by the SC TRIMH COBRE grant P20GM121342 at Clemson University. The views expressed in the article do not necessarily represent the views of the U.S DOE, NIH, or the United States Government.

REFERENCES

[1] Gailey, R., & Allen, K. (2008). Review of secondary physical conditions associated with lower-limb amputation and long-term prosthesis use. *Journal of Rehabilitation Research and Development, 45*(1), 15-30.

[2] Raichle, K., Hanley, M., Kadel, N., Campbell, K., Phelps, E., & Smith, D. (2008). Prosthesis use in person with lower and upper-limb amputation. *Journal of Rehabilitation Research & Development, 45*(7), 961-972.

[3] Robbins, C. B., Vreeman, D. J., Sothmann, M. S., Wilson, S. L., & Oldridge, N. B. (2009). A Review of the Long-Term Health Outcomes

Associated With War-Related Amputation. *Military Medicine, 174*(6), 588-592.

[4] Pirouzi, G., Abu Osman, N. A., Eshraghi, A., Ali, S., Gholizadeh, H., & Wan Abas, W. (2014). Review of the Socket Design and Interface Pressure Measurement for Transtibial Prosthesis. *The Scientific World Journal, 2014*.

[5] Klute, G. K., Glaister, B. C., & Berge, J. S. (2010). Prosthetic Liners for Lower Limb Amputees: A Review of the Literature. *Prosthetics and Orthotics International, 34*(2), 146-153.

[6] Hachisuka, K., Nakamura, T., Ohmine, S., Shitama, H., & Shinkoda, K. (2001). Hygiene Problems of Residual Limb and Silicone Liners in Transtibial Amputees Wearing the Total Surface Bearing Socket. *Archives of Physical Medicine and Rehabilitation, 82*.

[7] Baars, E., & Geertzen, J. (2005). Literature review of the possible advantages of silicon liner socket use in trans-tibial prostheses. *Prosthetics and Orthotics International, 29*(1), 27-37.

[8] Zhang, M., & Lee, W. C. (2006). Quantifying the Regional Load-Bearing Ability of Trans-Tibial Stumps. *Prosthetics and Orthotics International, 30*`(1), 25-34.

[9] Jia, X., Zhang, M., & Lee, W. C. (2004). Load transfer mechanics between trans-tibial prosthetic socket and residual limb-dynamic effects. *Journal of Biomechanics, 37*, 1371-1377.

[10] Lenka , P. K., & Choudhury, A. R. (2011). Analysis of Trans Tibial Prosthetic Socket Materials Using Finite Element Method . *J. Biomedical Science and Engineering*, 762-768.

[11] Lin, C.-C., Chang, C.-H., Wu, C.-L., Chung, K.-C., & Liao, I.-C. (2004). Effects of Liner Stiffness for Trans-Tibial Prosthesis: A Finite Element Contact Model. *Medical Engineering & Physics , 26*, 1-9.

[12] Boutwell, E., Stine, R., Hansen, A., Tucker, K., & Gard, S. (2012). Effect of Prosthetic Gel Liner Thickness on Gait Biomechanics and Pressure Distribution within the Transtibial Socket . *JRRD*, 227-240.

[13] Armstrong, D., Peters, E., Athanastou, K., & Lavery, L. (1998). Is there a critical level of plantar foot pressure to identify patients at risk for neuropathic foot ulcertation. *J Foot Ankle Surgery*, 303-307.

[14] Muller , M. J., Zou, D., & Lott, D. J. (2005). "Pressure Gradient" as an Indicator of Planta Skin Injury. *Diabetes Care*, 2908-2912.

[15] Johnson, K. (1987). *Contact Mechanics.* Cambridge, UK: Cambridge University Press .

[16] Sanders , J., Daly, C., Cummings, W., Reed, R., & Marks, R. (1994). A measurement device to assist amputee prosthetic fitting . *Journal of Clinical Engineering* , 63-71.

[17] Sanders, J. E., Greve, J. M., Mitchell, S. B., Zachariah, & Santosh, G. (1998). Material properties of commonly-used interface materials and their static coefficients of friction with skin and socks. *Journal of Rehabilitation Research and Development, 35*, 161-176.

[18] Kristinsson, O. (1993). The ICEROSS concept: a discussion of a philosophy. *Prosthetics and Orthotics International, 17*, 49-55.

[19] Sanders, J. E., Nicholson, B. S., Zachariah, S. G., Cassisi, D. V., Karchin, A., & Fergason, J. R. (2004). Testing of Elastomeric Liners Used in Limb Prosthetics: Classification of 15 Products by Mechanical Performance . *Journal of Rehabilitation Research & Development* , 175-186.

[20] Hafner, B. J., Cagle, J., Allyn, K. J., & Sanders, J. E. (2017). Elastomeric Liners for People with Transtibial Amputation: Survey of Prosthetists' Clincal Practices . *Prosthetics and Orthotics International*, 149-156.

[21] Pendry, J. B. (2000). Negative Refraction Makes a Perfect Lens. *Physical Review Letters*, 3966-3969.

[22] Shelby, R. A., Smith, D. R., & Schultz, S. (2001). Experimental Verification of a Negative Index of Refraction. *Science*, 77-79.

[23] Smith, D. R., Pendry, J. B., & Wiltshire, M. C. (2004). Metamaterials and negative refraction index. *Science*, 788-792.

[24] Cai, W., & Shalaev, V. (2010). *Optical Metamaterials: Fundamentals and Applications.* New York: Springer.

[25] Marques, R., Martin, F., & Sorolla, M. (2011). *Metamaterials with negative parameters: Theory, design and microwave applications.* New Jersey: John Wiley & Sons.

[26] Lv, C., Krishnaraju, D., Konjevod, G., Yu, H., & Jiang, H. (2014). Origami Based Mechanical Metamaterials . *Scientific Reports*, 1-6.

[27] Yu, X., Zhou, J., Liang, H., Jiang, Z., & Wu, L. (2018). Mechanical Metamaterials associated with stiffness, rigidity and compressibility: A brief review. *Progress in Materials Science*, 114-173.

[28] Cagle, J. C., Reinhall, P. G., Hafner , B. J., & Sanders, J. E. (2017). Development of Standardized Material Testing Protocols for Prosthetic Liners. *Journal of Biomechanical Engineering* .

[29] Lee, W. C., Zhang, M., Jia, X., & CHeung, J. T. (2004). Finite element modeling of the contact interface between trans-tibial residual limb and prosthetic socket. *Medical Engineering & Physics*.

[30] Cagle, J. C., Reinhall, P. G., Allyn, K. J., McLean, J., Hinrichs, P., Hafner, B. J., & Sanders , J. E. (2018). A Finite Element Model to Assess Transtibial Prosthetic Sockets with Elastomeric Liners . *Medical & Biological Engineering & Computing* , 1227-1240.

[31] Zhang, M., Lord, M., Turner-Smoth, A. R., & Roberts, V. C. (1995). Development of a non-linear Finite Element Modelling of the Below-knee prosthetic socket interface . *Medical Engineering & Physics* , 559-566.

[32] Steer, J. W., Worsley, P. R., Browne, M., & Dickinson, A. S. (2019). Predictive Prosthetic Socket Design: Part 1- Population-Based Evaluation of Transtibial Prosthetic Sockets by FEA-Driven Surrogate Modelling . *Biomechanics and Modeling in Mechanbiology*.

[33] Dickinson, A. S., Steer, J. W., & Worsley, P. R. (2017). Finite element analysis of the amputated lower limb: A systematic review and recommendations. *Medical Engineering & Physics, 43*(5), 1-18.

[34] Silver-Thorn, M. B., & Childress, D. S. (1995). Parametric Analysis Using the Finite Element Method to Investigate Prosthetic Interface Stresses for Persons with Trans-tibial Amputation. *Journal of Rehabilitation Research and Development* , 227-238.

[35] John DesJardins, Scott Edward Stanley, Breanne Przestrelski, Timothy C. Pruett, Steve L. Hoeffner, Brian Daryl Kaluf, "Variable Hardness Orthotic", Patent 10244818 B2, Publication 2019-04-02

[36] Przestrselski, B. T. (2017). *In-Shoe Innovation: 3-D Printed Foot Orthotses.* Clemson: Clemson University.

[37] O.H. Yeoh. (1993). Some forms of the strain energy function for rubber. Rubber Chem. Technol., 66:745–771.

[38] McGrath, M. P., Gao, J., Tang, J., Laszczak, P., Jiang, L., Moser, D., & Zahedi, S. (2017). Development of A Residuum/Socket Interface Simulator for Lower Limb Prosthetics . *Engineering in Medicine, 231*(3), 235-242.

[39] Zhang, M., Turner-Smith, A., Roberts, V., & Tanner, A. (1996). Friction Action at Lower Limb/Prosthetic Socket Interface. *Medical Engineering and Physics* , 207-214.

[40] Martins, P., Natal Jorge, R. M., & Ferreira, J. M. (2006). A Comparative Study of Several Material Models For Prediction of Hyperelastic Properties: APSlication to Silicone-Rubber and Soft Tissues. *Strain, 42*, 135-147.

[41] Faustini, M. C., Neptune, R. R., & Crawford, R. H. (2005). The quasi-static response of compliant prosthetic sockets for transtibial amputees using finite element methods. *Medical Engineering and Physics*, 114-121.

[42] Satterfield Z, Kulkarni N, Fadel G, Li G, Coutris N, Castanier MP (2018). "Unit Cell Synthesis for Design of Materials with Targeted Nonlinear Deformation Response" *ASME. J. Mech. Des.*; 139(8)

[43] Yeung, L. F., Leung, A. K., Zhang, M., & Lee, W. C. (2013). Effects of long-distance walking on socket-limb interface pressure, tactile sensitivity and subjective perceptions of trans-tibial amputees. *Disability and Rehabilitation*, 888-893.

[44] Hanspal, R. S., Fisher, K., & Nieveen, R. (2003). Prosthetic Socket Fit Comfort Score. *Disability and Rehabilitation*, 1278-1280.

[45] Downic , W., Leatham, P., Rhind, V., Wright, V., Branco, J., & Anderson, J. (1978). Studies with Pain Rating Scales. *Annals of Rheumatic Diseases*, 378-381.

[46] Legro, M., Reiber, G., Smith, D., del Aguila, M., Larsen, J., & Boone, D. (1998). Prosthesis Evaluation Questionair for Persons with Lower Limb Amputations: Assessing Prosthesis-Related Quality of Life. *Archives of Physical Medicine and Rehabilitation*, 931-938.